Short Papers

Microwave Modeling of Optical Periodic Waveguides

THEODOR TAMIR, FELLOW, IEEE

Abstract—**A design procedure and experimental method is presented for modeling optical periodic waveguides by means of more convenient parallel-plate microwave configurations. These models are suitable for verifying the beam-coupling properties of dielectric gratings that operate in the fundamental TE_0 surface-wave mode. In particular, blazed gratings with high coupling efficiencies have been constructed and their characteristics have been measured. The results have shown that previously developed design criteria, which are based on a simple Bragg-scattering approach, can yield highly efficient broad-band beam couplers that are not subject to critical fabrication tolerances.**

I. Introduction

Periodic waveguides in the form of thin film dielectric gratings deposited on thick substrates have been used [1] to couple optical surface waves into outgoing leaky-wave beams. However, the accurate measurement of their field properties is difficult to carry out at optical frequencies because of the small wavelengths involved. The purpose of this paper is to show that, by scaling down to microwave frequencies, models of optical dielectric gratings can easily be designed and constructed, so that their leaky-wave operation can be verified and their beam-coupling efficiency can be measured with great accuracy. An additional advantage of microwave models is that the grating profile can easily be modified to explore dispersion over a broad frequency spectrum.

When incident on a dielectric grating, a surface wave is converted into a leaky wave that accounts for two beams, of which one radiates in the region (usually, air) above the grating and the other into the substrate region. Because only the beam in the upper region is usually needed, the substrate beam represents an undesirable loss. Previous studies have shown [1]–[3] that energy is about evenly divided between the substrate and air beams if the grating has a symmetric profile (e.g., rectangular or sinusoidal) so that the theoretical coupling efficiency is around 50 percent. However, the unwanted beam can be suppressed and the coupling efficiency can thus be substantially increased [2]–[9] by using gratings having suitable asymmetrical profiles, which are referred to as "blazed" gratings in the optical literature. While such dielectric gratings have already been studied [10], their practical implementation has been slow because of difficulties in constructing accurate asymmetrical profiles at optical wavelengths. By utilizing microwave models instead, the present work has verified that efficient grating couplers can be constructed so that they are insensitive to stringent tolerance requirements. As anticipated in a preliminary note [11], the present results are consistent with an approximate Bragg-scattering approach to the scattering properties of blazed gratings having triangular or trapezoidal profiles [9], as well as with an exact analysis of the pertinent boundary-value problem of such gratings [10].

Manuscript received November 18, 1980; revised April 1, 1981. This work was supported by the National Science Foundation under Grant ENG77-28317, and by the Joint Services Electronics Program under Contract F49620-78-C-0047.

The author is with the Department of Electrical Engineering and Computer Science, Polytechnic Institute of New York, Brooklyn, NY 11201.

II. Analytical Considerations

The geometry of a typical blazed grating for use in integrated optics is shown in Fig. 1(a), where the refractive indices n_i (with $i=a, r, f$, and s) designate the air, periodic layer, waveguiding film, and substrate regions, respectively. When regarded as a beam coupler, the grating portion actually extends only to the right of some plane $x=x_0$; to the left of that plane, the periodicity is absent, i.e., $t_g=0$, and the layer of thickness t_f acts as a planar waveguide, which supports a surface wave characterized by a propagation constant β_{sw}. For incidence from the left as shown, the periodicity at $x>x_0$ transforms the incoming surface-wave field into a leaky wave that may generally account for several outgoing beams in the air and substrate regions [3].

The leaky-wave field consists of space harmonics varying as $\exp[j(\omega t-k_{xn}x)]$, where

$$k_{xn}=\beta_0+\frac{2n\pi}{d}-j\alpha \qquad (n=0,\pm1,\pm2\cdots) \tag{1}$$

and a two-dimensional situation ($\partial/\partial y\equiv 0$) is assumed. In practice, the leakage factor satisfies $\alpha\ll\beta_0$, while $\beta_0\simeq\beta_{sw}$. Also, the periodicity d is chosen so that a single diffraction order propagates, i.e., only the $n=-1$ component propagates to form a single outgoing beam in each of the air and substrate regions. The partition of energy between the two beams can then be expressed by the fractional powers (or coupling efficiencies) η_a and η_s for the air and substrate beams, respectively, which satisfy

$$\eta_a+\eta_s=1. \tag{2}$$

To maximize the coupling efficiency into the air beam, it is required to suppress the substrate beam and thus obtain $\eta_a\to 1$ (i.e., 100-percent coupling efficiency) as $\eta_s\to 0$. To achieve this aim, it is necessary to know η_a in terms of the grating parameters. While it is possible to obtain η_a by solving the pertinent boundary-value problem [10], such solutions are cumbersome and require time-consuming numerical computations if accurate quantitative data is needed. For design purposes, however, Chang and Tamir have developed [9] a simplified approach outlined below.

Recognizing that the outgoing beams are due to the scattering of energy by the oblique facets of the blazed grating, we consider the two sets of parallel planes inclined at the angles γ_1 and γ_2 with respect to the z-axis. In particular, as shown in Fig. 1(b), the set of planes inclined at γ_1 scatter the incident flux by reflection so that the partial contributions from the various planes interfere with each other. For constructive interference, the total electrical length of the segments AB and BC must equal 2π, which yields a generalized Bragg condition

$$\beta_{sw}d+k_0n_gd\cos 2\gamma_1=2\pi \tag{3}$$

where $k_0=2\pi/\lambda$, λ is the wavelength in air and n_g is an average

0018-9480/81/0900-0979$00.75 ©1981 IEEE

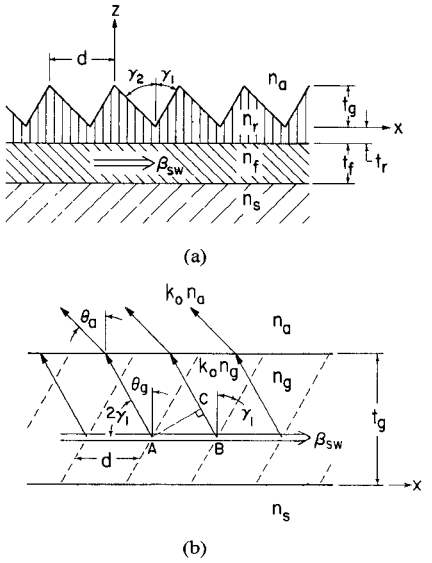

Fig. 1. Surface-wave scattering by a blazed grating. (a) Typical grating configuration. (b) Scattering of the incident energy by the set of grating facets that are inclined at the angle γ_1.

refractive index inside the periodic region, as defined by

$$n_g^2 = \epsilon_g = \frac{1}{t_g d}\int_0^{t_g} dz \int_0^d \epsilon(x,z)\,dx. \tag{4}$$

Here $\epsilon(x,z)=\epsilon(x+d,z)$ is the function describing the dielectric constant, so that ϵ_g is the (volume) average of that constant inside the periodic region.

For the situation shown in Fig. 1, condition (3) for γ_1 applies to a beam at an angle θ_a in the air and a similar condition holds for γ_2, which then accounts for a substrate beam. To suppress the latter beam, only condition (3) need be satisfied, while γ_2 should be taken so as to produce destructive interference. This can be most conveniently achieved [9] by choosing a right-angled triangular shape having

$$\gamma_2 = 0 \tag{5}$$

so that $\gamma_1=\gamma_B$ is then given from (3) and (5) by

$$\tan\gamma_B = \frac{d}{t_g} = \left(\frac{n_g+N-\lambda/d}{n_g-N+\lambda/d}\right)^{1/2} \tag{6}$$

where $N=\beta_{sw}\lambda/2\pi$ is the effective refractive index of the optical waveguide.

While (5) and (6) represent a simple design criterion for providing values of $\eta_a \simeq 1.0$ and $\eta_s \simeq 0$, it is important for practical purposes to know how critical these conditions are. A consideration of the stop bands associated with the periodic layer in Fig. 1(b) then shows [9] that good blazing ($\eta_a \geqslant 0.9$) is maintained even if incremental changes occur in the grating parameters, provided that such changes fall within a range defined by

$$-1 \leqslant \frac{4}{n_r^2-n_a^2}\frac{\lambda}{d}\Delta\left(\frac{n_g^2 d}{\lambda}\cos^2\gamma_1\right) \leqslant 1. \tag{7}$$

Here $\Delta(u)$ refers to the increment in the variable u with respect to its value at $\gamma_1=\gamma_B$. Thus, when only $\lambda=c/f$ changes, (7) defines a frequency band Δf given by

$$\frac{\Delta f}{f} = \pm\frac{n_r^2-n_a^2}{(2n_g\cos\gamma_B)^2} \tag{8}$$

and similar results hold if one of the other parameters varies. Condition (7) therefore provides fabrication tolerances with respect to the design-center values, whereas (8) specifically yields the frequency band for good blazing properties, i.e., for effective suppression of the substrate beam.

III. Modeling Considerations

Due to fabrication and/or mechanical constraints, optical gratings usually involve the four different dielectric media shown in Fig. 1(a). At microwaves, however, it is possible to use a simplified model consisting of a single dielectric material, with air occupying both the upper and lower open ranges, i.e., $n_r=n_f$ and $n_s=n_a=1$.

The modeling considerations are then sketched in Fig. 2, where the simplified grating geometry is indicated in Fig. 2(a). The incident surface wave assumed in both Figs. 1 and 2(a) is the fundamental TE_0 mode, whose electric field is parallel to the y axis and varies as shown in Fig. 2(b). It is therefore possible to place metallic walls as shown in Fig. 2(b), so that the TE_0 surface wave becomes the fundamental TE_{00} mode inside the parallel-plate system. To ensure that higher order TE_m ($m\neq 0$) modes do not propagate, the overall grating thickness t_f+t_g is made small; also, by choosing the plate separation b to also be small enough, all higher order modes TE_{mn} (with $m, n\neq 0$) are below cutoff in the parallel-plate waveguide. In this manner, the field in that waveguide corresponds exactly to the surface wave (and hence to the leaky-wave fields) along the dielectric grating of Fig. 1(a).

To excite the TE_{00} mode, we then note from Fig. 2(c) that its field closely matches the TE_{10} mode in a conventional rectangular waveguide having a narrow side equal to the separation b between the parallel plates. Because of the dispersion relations pertinent to the waveguide TE_{10} mode and to the surface-wave TE_{00} mode, the second side a of the rectangular guide is larger than the thickness t_f+t_g of the dielectric grating. This further favors a good match because, in both cases, the field amplitude is largest and varies as a cosine in the central portion.

The considerations illustrated in Fig. 2 led to the X-band modeling implementation sketched in Fig. 3, where the x, y, z coordinates are oriented in the same fashion as in Figs. 1 and 2. The parallel-plate system consists of aluminum sheets separated by small polyfoam supports, with microwave power being fed via a conventional X-band flange. To provide a smooth transition from the TE_{10} waveguide mode first to the TE_{00} surface mode ($t_g=0$) and then to the leaky-wave field along the grating (t_g finite), the periodic portion is located far (about 10λ) from the flange connection. The dielectric waveguide and grating is made of teflon with $n_r=n_f=1.414$. To further improve the field match, the dielectric line is tapered at both ends, as indicated in Fig. 3 for the output portion. For clarity, the input taper is not shown; its length is about 5″ (over 4λ) and about half that length extends into the rectangular guide.

As the parallel-plate system is open with respect to the z direction, the field was probed along x with simple detectors. One detector on each one of the two sides was used, but only the right-hand detector is shown in Fig. 3. By placing the dielectric grating at the center of the parallel-plate system and by using appropriate calibration, these detectors have provided the following data.

1) Field-strength readings on the two sides (right and left with respect to x); this yielded the power ratios η_a and η_s for the "air" and "substrate" regions, respectively.

2) Variation of the field amplitude as a function of x; as this

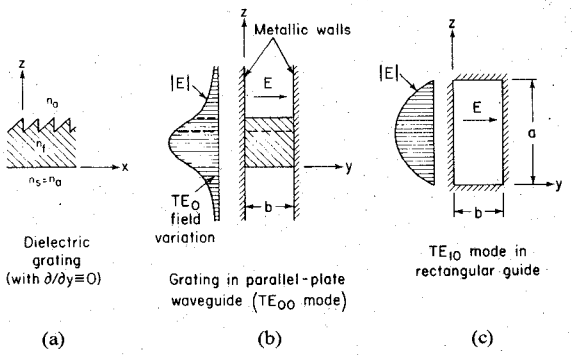

Fig. 2. Considerations for microwave modeling. (a) Simplified grating geometry. (b) Field variation and placement of grating inside a metallic parallel-plate waveguide. (c) Field variation in rectangular waveguide used to excite the mode in (b).

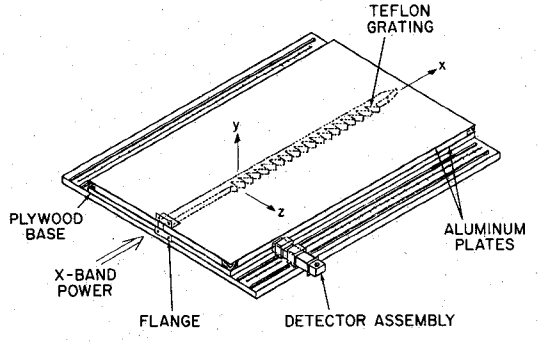

Fig. 3. Parallel-plate setup for measuring the fields supported by grating structures.

variation agreed well with the expected $\exp(-\alpha x)$ leaky-wave behavior, the value of α was easily extracted from the measured data.

Such measures were taken for several teflon gratings, with typical results being discussed below.

IV. Theoretical and Experimental Results

Based on the above modeling considerations, the teflon waveguides can be built by first choosing a thickness t_f so as to support a single surface wave and then designing the appropriate grating profile prescribed by (5) and (6). Relations (7) and (8) then assess the frequency bandwidth and the geometrical tolerances allowable for good blazing performance ($\eta_a \geq 0.9$). The parallel-plate setup of Fig. 3 can experimentally verify the actual value of η_a and it can also provide the leakage parameter α which is not given by the Bragg-scattering analysis of Section II. While this procedure was applied in the present case, for which $f=10$ GHz was used as the center-design frequency, exact values of both η_a and α have also been separately found by a numerical evaluation of a theoretical solution [10] of the pertinent boundary-value problem.

Typical examples are shown in Fig. 4 for two separate gratings that differed only in their tooth height t_g, both being characterized by an effective refractive index $N=1.097$ at 10 GHz. For the entire X-band, the periodicity $d=1.75$ cm then satisfied $|k_{x,-1}|<k_0$ and $|k_{xn}|>k_0$ for all $n\neq -1$, thus ensuring that only the $n=-1$ space harmonic propagates, as discussed after relation (1). In this case, the leaky-wave radiates in the backward direction, as is also suggested in Fig. 1(a). The height $t_g=3.04$ cm of the larger grating was chosen to comply with conditions (5) and (6) at 10 GHz. We then notice from Fig. 4 that this larger grating

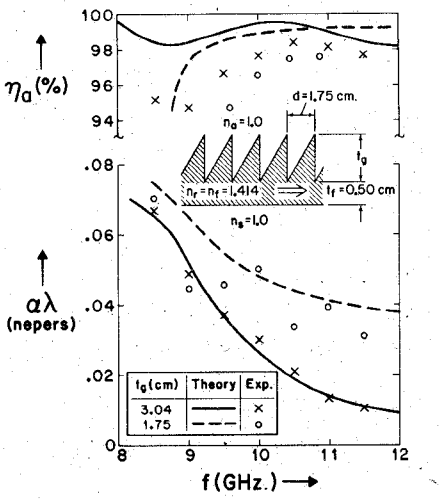

Fig. 4. Efficiency η_a and normalized leakage $\alpha\lambda$ as a function of frequency f, for two blazed dielectric gratings.

shows an excellent agreement between the theoretical result [10] shown by the solid curve, and the experimental data shown by crosses. In particular, the theoretical value of η_a at 10 GHz is 99.5 percent while the experimental result is 97.7 percent, with a peak of 98.4 percent measured at 10.5 GHz. More importantly, all measured values of η_a are higher than 94 percent over the entire frequency band under consideration. In fact, relation (8) yields $\Delta f/f=\pm 0.22$, which specifies a range $7.8\leq f\leq 12.2$ GHz. Thus while the measurements could cover only about 3/4 of that range, they have verified well the effectiveness of the Bragg-scattering approach that led to relations (5)–(8).

To check the sensitivity of η_a on the grating parameters, a second grating with smaller $t_g=1.75$ cm was measured, as shown in Fig. 4 by the dashed curves for theoretical results and by the dots for the measured data. Based on relation (7), this large change in t_g is still within the range allowed for good blazing operation. While Fig. 4 shows that the efficiency η_a for such a grating deteriorates at the lower frequencies, the predicted good blazing behavior at the center frequency is confirmed. In fact, the pertinent theoretical result is $\eta_a=98.8$ percent while the experimental data is 96.5 percent at $f=10$ GHz, with even higher values at the higher frequencies.

To further check the sensitivity of η_a on the grating parameters, the upper portions of the grating teeth were machined down, thus leading to trapezoidal shapes as shown in Fig. 5. In this case, the design criteria (5) and (6) are not changed, except that now n_g varies with t_g according to (4), which yields

$$n_g^2=n_{g0}^2+\frac{n_r^2-n_a^2}{2}\left(1-\frac{t_g}{t_{g0}}\right) \tag{9}$$

where the second subscript 0 denotes values at the design center, i.e., before the teeth have been decreased in height. Inserting this into (7) and using the equal sign therein, one gets

$$\frac{t_g}{t_{g0}}=\frac{1}{1+\cos^2\gamma_B} \tag{10}$$

where now t_g refers to the minimum value that still satisfies (7). For the grating with $t_{g0}=3.04$ cm in Fig. 5, one then obtains $t_g/t_{g0}=0.57$, for which η_a is predicted by exact calculations [10] to be 98.5 percent. A closely measured result is 97.2 percent and, furthermore, we observe that the measured data of η_a are larger

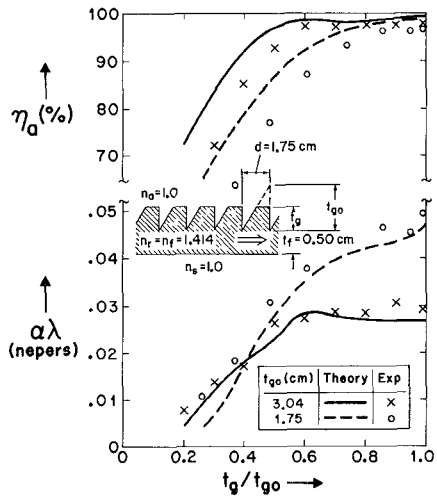

Fig 5. Efficiency η_a and normalized leakage $\alpha\lambda$ as a function of the normalized grating height t_g/t_{g0} obtained by cutting the teeth of the gratings in Fig 4 All data are shown for f=10 GHz

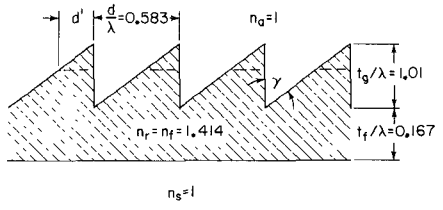

Changing parameter	INCREMENTS		
	Bragg analysis	Exact analysis*	Measured*
λ	22%	>20%	>20%
d	22	>20	N A
t_g	29	48	(>50)
$n_g(d')$	7	11	9

*for η_a=0 9

Fig 6. Summary of results showing increments allowed in the grating parameters λ, d, t_g, and n_g. In most cases, the increments noted in the table refer to both positive (increasing) and negative (decreasing) quantities.

than 90 percent for all $t_g/t_{g0}>0.45$. As in Fig. 4, theoretical results for the larger grating are shown in Fig. 5 by solid curves, while measured data are given by crosses.

The grating with smaller $t_{g0}=1.75$ cm has been similarly measured, as also shown in Fig. 5. As expected, the blazing performance (shown by dashed lines and by dots) now deteriorates more rapidly as t_g is reduced because this grating does not satisfy the Bragg condition (6) even at $t_g=t_{g0}$. Nevertheless, the smaller grating shows measured values of $\eta_a>90$ percent for $t_g/t_{g0}>0.62$, thus confirming well the large permissible tolerances predicted by condition (7).

In both Figs. 4 and 5, the measured values of η_a are smaller than the theoretical ones, but this is due to unavoidable stray radiation and to scattering from discontinuities; this scattering produces detected fields that are somewhat stronger than those in a truly open geometry such as that of Fig. 1(a). As a result, the weaker field in the "substrate" was relatively more affected than that in the "air" region, so that the measured value of η_a was smaller than that obtained in the absence of stray scattering. By inserting suitably placed absorbers inside the parallel-plate system, this deleterious effect was substantially reduced but it was impossible to suppress it completely.

To further explore the sensitivity of η_a on the grating parameters, other grating configurations were constructed and measured, with most of the relevant measurements being summarized in Fig. 6. Changes of λ and d are equivalent and increments in these quantities were restricted to 20 percent because larger values may introduce higher order modes and/or more than a single outgoing beam in the outer regions. The increment for t_g indicated by (>50 percent) in Fig. 6 is shown in brackets because it represents only a conservative estimate based on measurements for which η_a was actually larger than 90 percent. The change in $n_g=n_g(d')$ refers to that illustrated in Fig. 5.

The results summarized in Fig. 6 indicate that the design criteria embodied in relations (5)–(8) are fully confirmed by teflon gratings. However, theoretical results show [9], [10] that they hold also for other dielectric materials and different configurations. This suggests that the present verification applies to a wider class of grating structures.

V. Conclusions

The present work has shown that it is possible to model optical periodic waveguides by analogous microwave configurations which can more readily serve to measure pertinent electromagnetic properties. In general, the present study has confirmed the validity of simple design criteria that are based on a Bragg-scattering interpretation of the grating operation; while these criteria are consistent with accurate data obtained by more sophisticated but cumbersome analytical methods, they have now been shown to agree well with experimental results. In particular, the microwave models of optical gratings have demonstrated the possibility of constructing blazed grating couplers that enhance the beam in the air region at the expense of the beam in the substrate, thus achieving a very high coupling efficiency. These couplers exhibit broad frequency band characteristics and are not subject to stringent fabrication tolerances.

Acknowledgment

The author wishes to acknowledge the able assistance of A. Gruss and K. T. Tam in carrying out the experimental work, and of V. Shah in providing the numerical results. Special thanks are due to Mrs. A. Nattboy for her very reliable and neat effort in typing this manuscript.

References

[1] T. Tamir, "Beam and waveguide couplers," in *Integrated Optics*. Berlin, Germany: Springer-Verlag, 1979, ch. 3, p. 84.
[2] W. Streifer, R. D. Burnham, and R. D Scifres, "Analysis of grating-coupled radiation in GaAs:GaAlAs lasers and waveguides," *IEEE J. Quant. Electron*, vol. QE-12, pp. 422–428, July 1976, and pp. 494–499, Aug 1976.
[3] T. Tamir and S. T Peng, "Analysis and design of grating couplers," *Appl. Phys*, vol. 14, pp. 235–254, Nov 1977.
[4] S. T Peng and T. Tamir, "Directional blazing of waves guided by asymmetric dielectric gratings," *Optics Commun.*, vol 11, pp. 405–409, Aug. 1974.
[5] T Aoyagi, Y Aoyagi, and S. Namba, "High efficiency blazed grating couplers," *Appl Phys Lett.*, vol. 29, pp. 303–304, Sept. 1976.
[6] D. Marcuse, "Thick dielectric grating on asymmetric slab waveguide," *Bell Syst. Tech. J.*, vol. 56, pp. 329–353, March 1977.
[7] K. C. Chang and T. Tamir, "Bragg-reflection approach for blazed dielectric gratings," *Optics Commun.*, vol. 26, pp 327–330, Sept 1978
[8] W H. Lee and W Streifer, "Radiation loss calculation for corrugated dielectric waveguides," *J Opt. Soc Amer.*, vol. 68, pp 1701–1707, Dec 1978; and vol. 69, pp. 1671–1676, Dec. 1979
[9] K. C. Chang and T. Tamir, "Simplified approach to surface-wave scattering by blazed dielectric gratings," *Appl. Optics*, vol 19, pp 282–288, Jan. 1980.

[10] K. C. Chang, V. Shah, and T. Tamir, "Scatterings and guiding of waves by dielectric gratings with arbitrary profiles," *J. Opt. Soc. Amer.*, vol. 70, pp. 804–813. (Refer to the bibliography therein for other solution methods.)
[11] A. Gruss, K. T. Tam, and T. Tamir, "Blazed dielectric gratings with high beam-coupling efficiencies," *Appl. Phys. Lett.*, vol. 36, pp. 523–525, Apr. 1980.

Anomalous Low-Loss Transmission in a Gas-Confined Dielectric Waveguide for Millimeter and Submillimeter Wavelengths

KAZUYUKI YAMAMOTO, MEMBER, IEEE

Abstract— **A novel low-loss (gas-confined) dielectric waveguide for millimeter and submillimeter wavelengths was previously reported by the author. The waveguide consists of a thin dielectric tube separating an internal high-dielectric-constant gas from an external low-dielectric-constant gas. The attenuation constant of this form of waveguide usually increases with increasing tube thickness. The thick tube is indispensable for a mechanically stable waveguide. In this paper, anomalous low-loss transmission characteristics in a gas-confined dielectric waveguide with a thick tube are described. Some conditions are theoretically found where the attenuation constant of the waveguide with a thick tube is extremely low, due to tight field confinement within the internal gas. A qualitative explanation of the operation mechanism is also given.**

I. Introduction

Dielectric waveguides have received considerable interest in recent years for millimeter and submillimeter wavelengths transmission media. The advantage of the dielectric waveguides is that, in these wavelength regions, waveguide dimensions are of an order that can be easily fabricated and handled. However, the dielectric waveguide suffers from a fairly large attenuation. In order to bring the dielectric waveguide to practical use, it is most important to reduce transmission loss.

In designing a low-loss dielectric waveguide, two loss mechanisms, attenuation due to dielectric loss of materials and radiation loss from bends, should be simultaneously reduced. The transmission characteristics are closely dependent on waveguide field distribution. The attenuation of the dielectric circular rod waveguide is very small, if the wavefield energy exists almost entirely outside the dielectric rod [1]. A small curvature of the waveguide, however, will result in appreciable radiation losses. The attenuation is decreased at the expense of radiation loss.

To overcome these difficulties inherent in the dielectric waveguide, the author previously presented a novel approach to obtain a low-loss dielectric waveguide [2]. The waveguide consists of a thin dielectric tube which separates an internal high-dielectric-constant gas from an external low-dielectric-constant gas, as shown in Fig. 1. The characteristic feature of this waveguide is that the attenuation constant can be considerably reduced without incurring a radiation loss increase, because most of the power flows within the low-loss internal gas and not in the dielectric tube. The low-loss properties of the gas-confined dielectric waveguide have been demonstrated theoretically and experimentally.

Manuscript received November 18, 1980; revised April 16, 1981.
The author is with the Musashino Electric Communication Laboratory, NTT, Musashino-shi, Tokyo, 180 Japan.

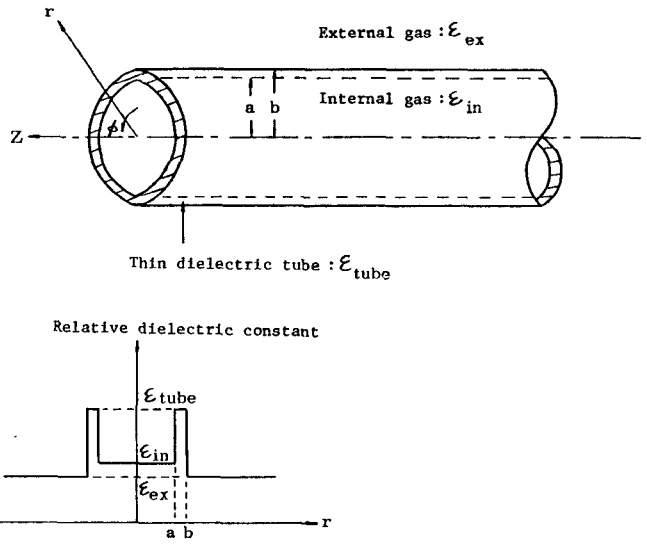

Fig. 1. Geometry and dielectric-constant profile of the gas-confined dielectric waveguide. The waveguide consists of a thin dielectric tube which separates an internal high-dielectric-constant gas from an external low-dielectric-constant gas.

Generally, gases, due to their low density, have much lower dielectric constants and much smaller absorption coefficients than solid dielectrics. If a dielectric tube is not so thin, most of the power is confined within the tube and not in the internal gas, and the waveguide suffers from a fairly large attenuation. The advantage of the gas-confined guide is brought about only when the tube is sufficiently thin. Thin dielectric tubes, however, involve problems with mechanical stability.

In this paper, the transmission characteristics of a gas-confined waveguide which consists of a relatively thick tube are presented. It is theoretically shown that there exist novel and anomalous conditions where most of the power travels within the internal gas and where propagation loss is extremely small. These phenomena were originally suggested by Marcatili [3]. His analysis was limited to extraordinary conditions. In this paper, the anomalous transmission characteristics are more accurately and clearly described.

II. Transmission Characteristics of Gas-Confined-Guide

The geometry and dielectric-constant profile of the gas-confined guide are shown in Fig. 1. Guided modes along the gas-confined guide can be analyzed in a standard manner. To clarify our results, discussions are limited to TE_{0n} modes propagation. Assuming a field with the time and z dependence of $e^{i(\omega t-\beta z)}$, axial field components of TE_{0n} modes can be expressed as follows:

$$H_z=\begin{cases} AI_0(\kappa r) \quad (\text{or } AJ_0(\kappa r)), & r\leq a \\ SJ_0(\sigma r)+TN_0(\sigma r), & a\leq r\leq b \\ CK_0(\gamma r), & b\leq r \end{cases} \tag{1}$$

0018-9480/81/0900-0983$00.75 ©1981 IEEE